AI and solar flares: prediction, representation, and interpretation of the main triggers of space weather

michele piana

MIDA, dipartimento di matematica, università di genova

INAF OATO, torino

COSPAR, athens 16-24 july 2022

INAF

ISTITUTO NAZIONALE DI ASTROFISICA
OSSERVATORIO ASTROFISICO DI TORINO

solar flares in space weather

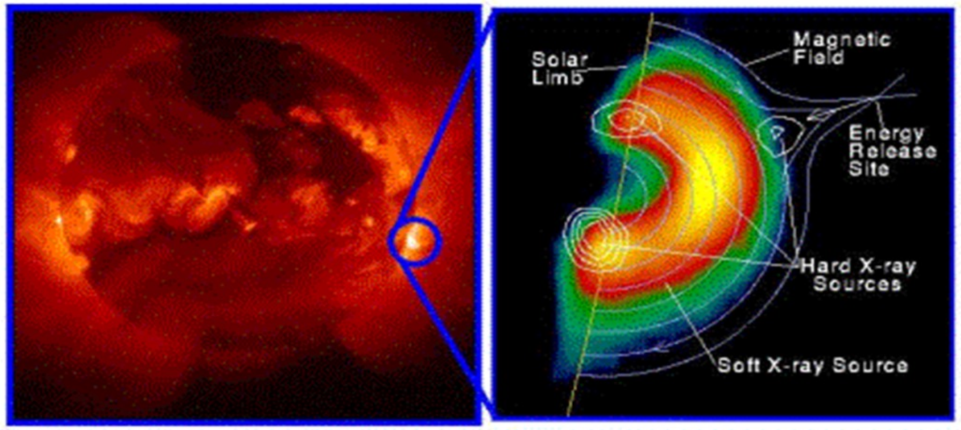

Yohkoh X-ray Image of a Solar Flare, Combined Image in Soft X-rays (left) and Soft X-rays with Hard X-ray Contours (right). Jan 13, 1992.

- extend over 10,000 kilometers
- release more than 10^{32} ergs in 10-100 seconds
- accelerate billion tons of material to more than a million km per hour
- produce electromagnetic radiation at all wavelengths
- **are the main trigger of space weather**

the flare paradox

high resistance + low inductance = short time for current to flow

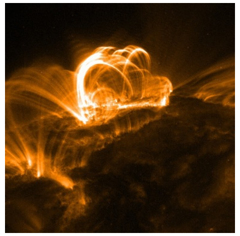

low resistance + high inductance = (impossibly) long time for current to excite the flare

interpretation of solar flares

- two possible perspectives:
  - triggered by magnetohydrodynamics: numerical solution of MHD PDEs
  - **triggered by data: AI for identification of patterns in the data mess**

- **AI and solar flares:**
  - **machine learning for flare prediction**
  - **desaturation for EUV imaging**
  - **inversion methods for hard X-ray imaging**

solar flare forecasting – the feature-driven supervised approach

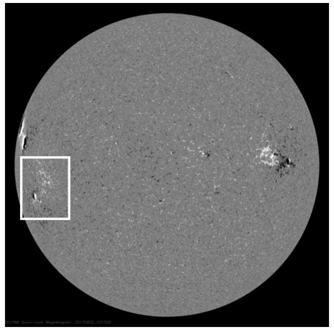

historical data set:
the HMI archive

Q1: is a warning machine for a flaring storm possible?

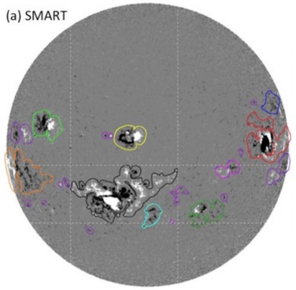

features extraction:
FLARECAST

Q2: which features mostly impact the flare forecasting effectiveness?

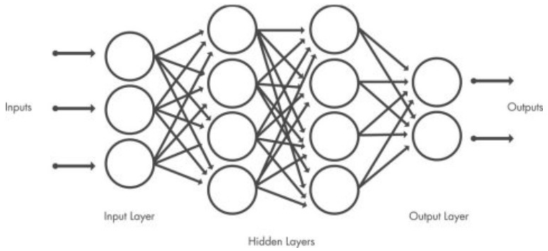

supervised machine learning:
hybrid LASSO

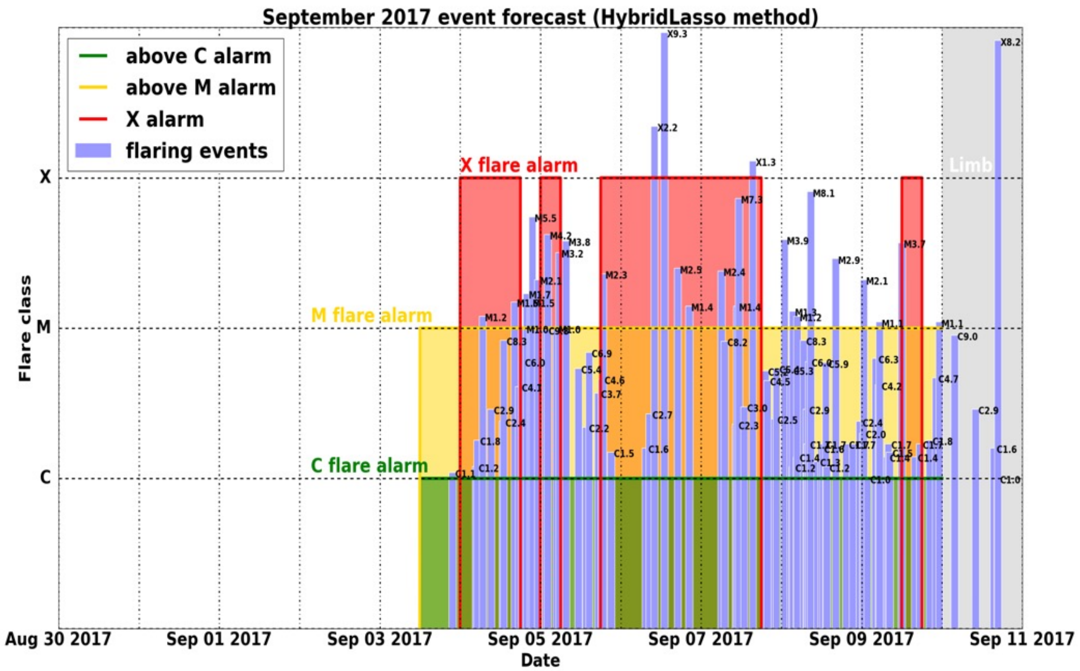

feature	rank (mean)	rank (standard deviation)
2 ↑	2,5	2,4
3 ↑	3,5	2,4
4 ↑	4,5	2,4
1 ↓	5	1
5 ↔	5,5	2,4
11 ↑↑	7,3	6,7
6 ↓	7,3	4,2
7 ↓	7,3	1,9
8 ↓	7,5	1,7
9 ↓	8,3	1,9
12 ↑	10,8	0,9
13 ↑	11,8	0,9
10 ↓	12	6
14 ↔	12,8	0,9
15 ↔	14,3	0,5
16 ↔	16	0
17 ↔	17	0
18 ↔	18	0
19 ↔	19	0
20 ↔	20	0
21 ↔	21	0
22 ↔	22	0
23 ↔	23	0

forecasting the september 2017 flaring storm

- (benvenuto, campi, massone, piana; 2020; astrophysical journal letters)

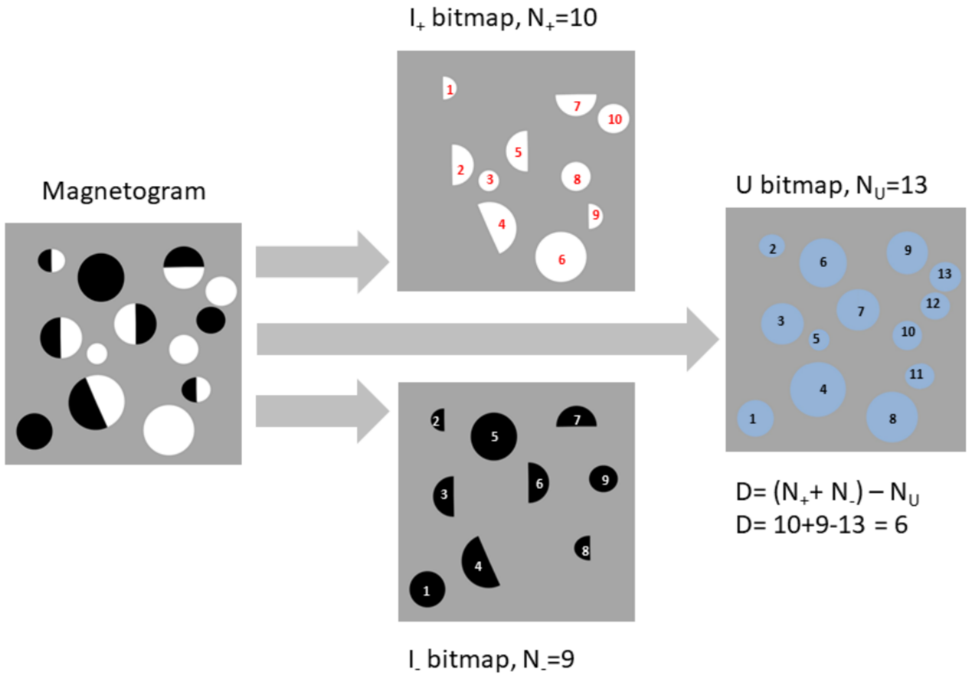

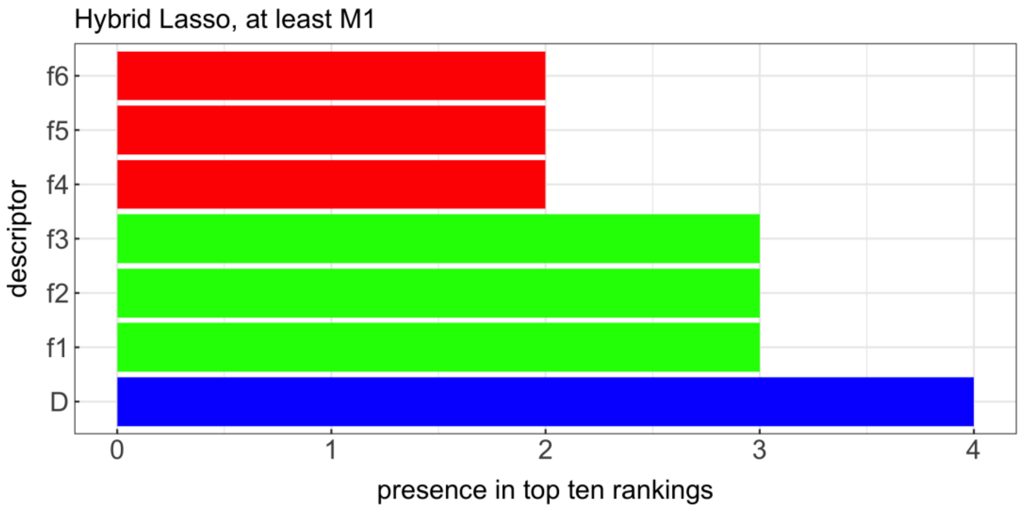

a new topological descriptor

- (cicogna et al, *ApJ*, 2021)

video-based deep learning (guastavino et al, *A&A*, 2022)

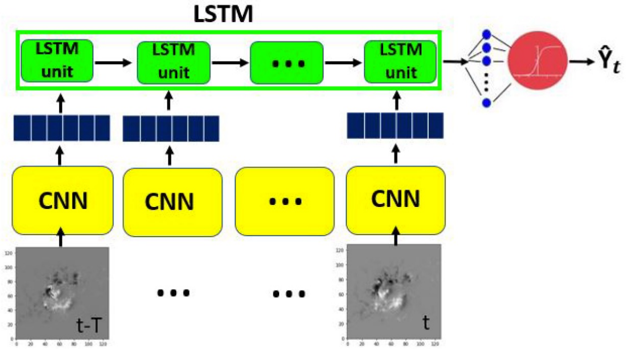

(a) LRCN architecture

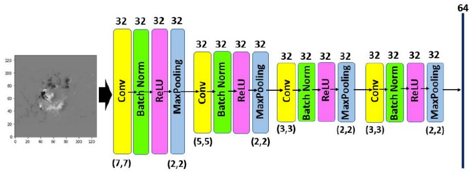

(b) CNN architecture

	TSS (C1+ flares)						
	Mean	Std	Min	25th perc	Median	75th perc	Max
Validation	0.57	0.02	0.55	0.56	0.57	0.59	0.61
Test	0.55	0.05	0.46	0.52	0.54	0.60	0.61
	TSS (M1+ flares)						
	Mean	Std	Min	25th perc	Median	75th perc	Max
Validation	0.76	0.07	0.65	0.67	0.77	0.82	0.85
Test	0.68	0.09	0.55	0.61	0.69	0.72	0.82

flare morphology at EUV wavelengths

AI and solar flares: desaturation of EUV images

data: atmospheric imaging assembler in the solar dynamics observatory (SDO/AIA)

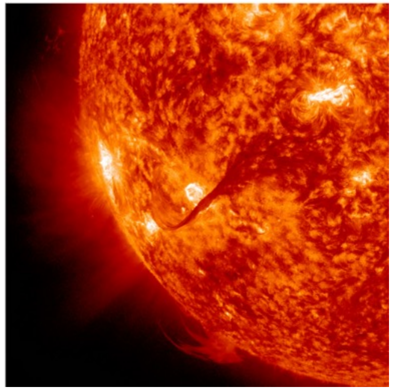

- four telescopes
- seven EUV wavelengths
- 1.5'' spatial resolution
- 12 s time cadence

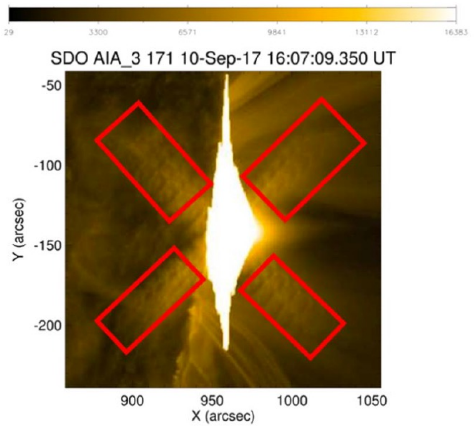

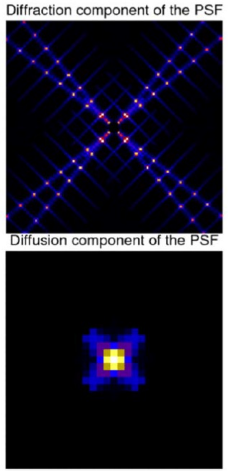

- **primary saturation:** the signal generated by the incoming photon flux exceeds the capacity of the CCD pixels (16383 DN pixel^{-1})
- **blooming:** exceeding charge spreads along the north-south direction
- the core PSF induces **diffusion** effects
- the **diffraction** PSF replicates at periphery the interaction between radiation and filters support

all information lost due to primary saturation is in the peripheral diffraction pattern
this information can be restored by solving an inverse diffraction problem

adaptive poisson related LASSO (april)

- refined segmentation of the saturation region
- weights according to the shape of the saturation region
- refined estimation of the saturated values for intense background

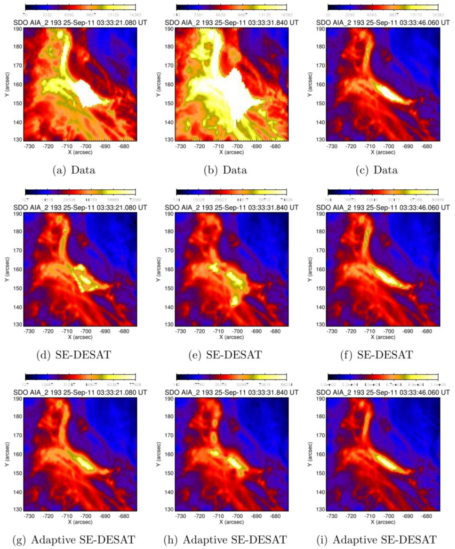

Algorithm 1. Adaptive SE-DESAT adaptive sparsity enhancing desaturation

1: Compute the saturated region I_S (see section 3.2.1)
2: Set $\mathbf{b} = \mathbf{0}_n$, $\hat{\mathbf{x}} = \mathbf{1}_p$ and compute the adaptive weights $\mathbf{w}$ (equation (50))
3: **repeat**
4: Update the background with a step of EM method
$$\mathbf{b} \leftarrow \mathbf{b} \, \frac{\mathbf{y}}{\mathbf{H}\hat{\mathbf{x}}+\mathbf{b}}$$
5: Compute the APRiL estimator $\hat{\mathbf{x}}^{\mathbf{w}}(\lambda)$ and the intercept $\alpha(\lambda)$, $\forall\lambda$ (equation (51))
6: Compute the optimal regularization parameter λ^* (see section 3.2.6)
7: Update the saturated region values and correct the background values
$$\hat{\mathbf{x}} \leftarrow \hat{\mathbf{x}}^{\mathbf{w}}(\lambda^*) \qquad \mathbf{b} \leftarrow \mathbf{b} + \alpha(\lambda^*)\sqrt{\mathbf{y}+1}$$
8: Correct the saturated region values by a threshold map $\mathcal{T}_{\overline{\alpha}}$ (equation (53))
9: **until** Test on the goodness of fit is satisfied (see section 3.2.7)
10: **return** the desaturated image $\hat{\mathbf{g}} = \mathcal{G}(\hat{\mathbf{x}})$ (see synthesis equation (58))

$$\hat{\mathbf{x}}^{\mathbf{w}}(\lambda) := \arg\min_{\mathbf{x}\in\mathbb{R}^p} \|\mathbf{y} - \mathbf{H}\mathbf{x} - \mathbf{b}\|_\Lambda^2 + \lambda \sum_{j\in I_S} w_j |\mathbf{x}_j|,$$

(guastavino et al, *ApJ*, 2019)

thermal vs non-thermal emission: the hard X-ray perspective

the STIX imaging concept

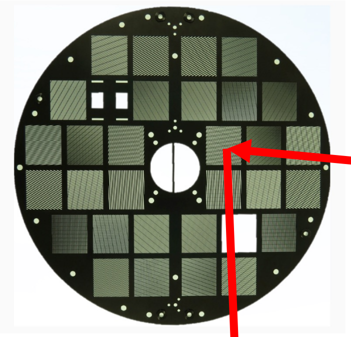

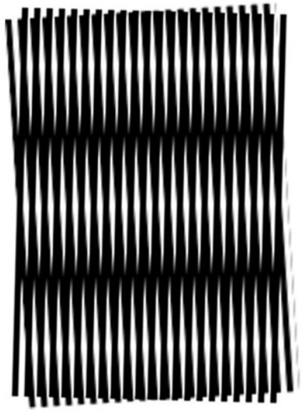

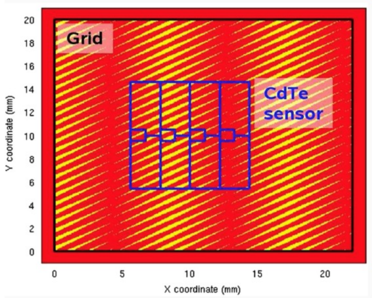

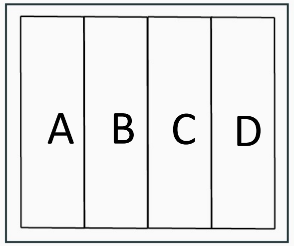

$$V(\xi) \simeq \frac{1}{4M_1}[(\boldsymbol{C} - \boldsymbol{A}) + i(\boldsymbol{D} - \boldsymbol{B})] \exp\left(i\frac{\pi}{4}\right)$$

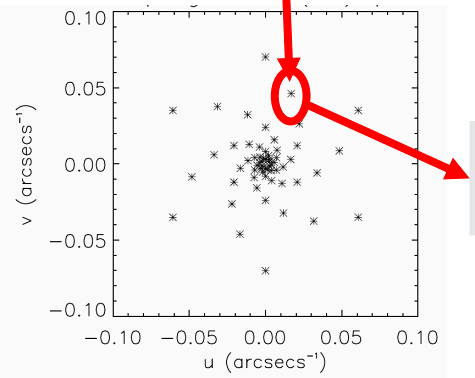

$$\xi = \mathbf{k}^f \frac{L_1 + L_2}{S} - \mathbf{k}^r \frac{L_2}{S}$$

$$V(\xi) = \int_{\mathbb{R}^2} \phi(\mathbf{x}) \exp(2\pi i \xi \cdot \mathbf{x})\, d\mathbf{x}.$$

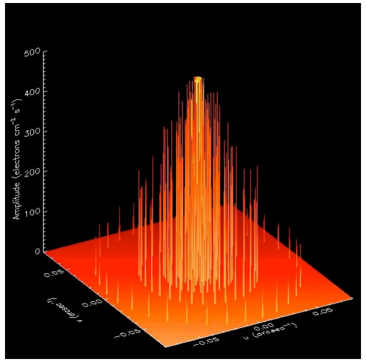

AI

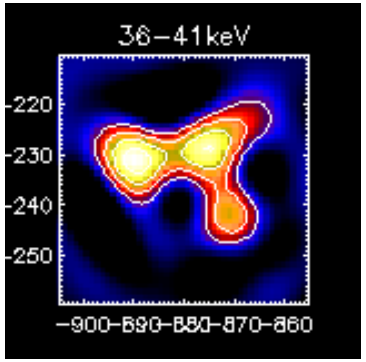

STIX: first images from fully calibrated visibilities

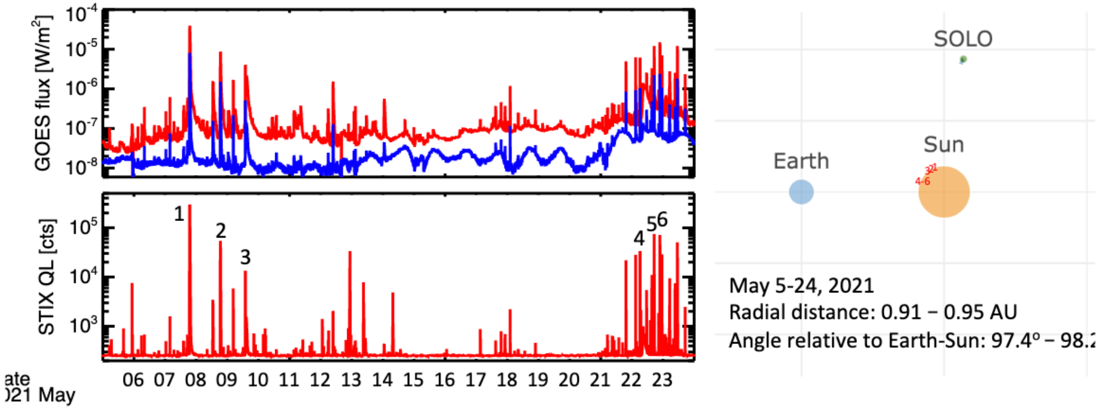

imaging method: MEM_GE (massa et al, *ApJ*, 2020)

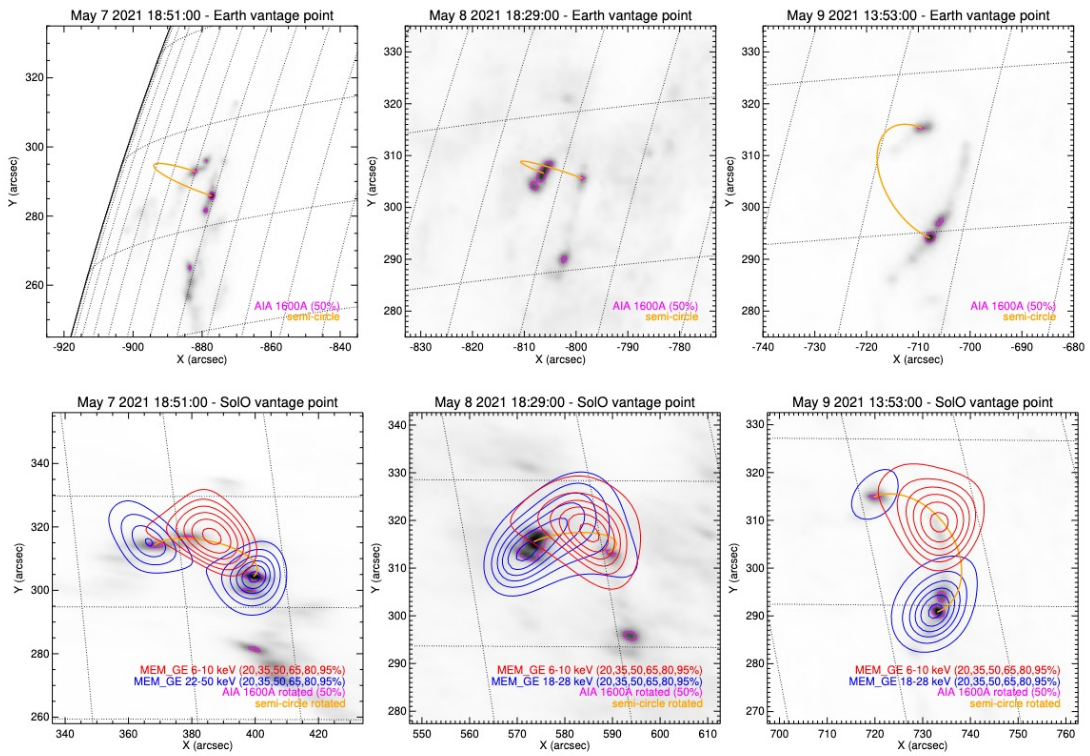

(massa et al, *solar physics*, submitted)

papers and codes

- **perracchione e, massa p, massone a m and piana m 2021** visibility interpolation in solar hard X-ray imaging: application to RHESSI and STIX *astrophysical journal* 919 133
- **massa p, perracchione e et al 2021** imaging from STIX visibility amplitudes *astronomy and astrophysics* **656** A25
- **cicogna d, berrilli f, calchetti d, del moro d, giovannelli l, benvenuto f, campi c, guastavino s and piana m 2021** flare forecasting algorithms based on high-gradient polarity inversion lines in active regions *astrophysical journal* **915** 38
- **battaglia a f et al 2021** STIX X-ray microflare observations during the solar orbiter commissioning phase *astronomy and astrophysics* **656** A4
- **guastavino s and benvenuto f 2020** a mathematical model for image saturation with an application to the restoration of solar images via adaptive sparse deconvolution *inverse problems* **37** 015010
- **benvenuto f, campi c, massone a m and piana m 2020** machine learning as a flaring storm warning machine: was a warning machine for the 2017 september solar flaring storm possible? *astrophysical journal letters* **904** L7
- **krucker s et al 2020** the spectrometer/telescope for imaging X-rays *astronomy and astrophysics* **642** A15
- **massa p, schwartz r, tolbert a k, massone a m, dennis b r, piana m and benvenuto f** 2020 MEM_GE: a new maximum entropy method for image reconstruction from solar x-ray visibilities *astrophysical journal* **894** 1
- **guastavino s et al** 2022 implementation paradigm for supervised flare forecasting studies: a deep learning application with video data *astronomy and astrophysics* **662** A105

most flare prediction codes art accessible at the github link: https://github.com/theMIDAgroup/AI-FLARES

STIX imaging codes are included in the HESSI GUI of SSW

projects

- HESPE, FP7
- FLARECAST, H2020
- AI-FLARES, ASI/INAF
- METIS-SWA-STIX instrutments, ASI/INAF
- SWESNET, ESA
- ARCAFF, HE